Improving the Robutness of T1 Mapping to Fat Partial Volume Effects

Inês Alexandra Margalho Carreiras
ines.carreiras@tecnico.ulisboa.pt

Instituto Superior Técnico, Universidade de Lisboa, Portugal

July 2021

Abstract

Cardiac magnetic resonance T1 mapping, which allows direct quantification of the myocardial signal, has been widely applied, as it enables the quantitative characterization of myocardial tissue in vivo in a non-invasively. However, this technique has been largely restricted to the left ventricle because of the partial volume effect related to relatively limited spatial resolution and motion-related artifacts. The aim of the present work is based on the investigation of the impact of the presence of fat infiltration in the tissue on the quantification of myocardial T1. The methodology adopted included the execution of signal simulations of T1 inversion-recovery mapping sequences with a balanced Steady-State Free Precession (bSSFP) readout using the MATLAB® software. To validate the simulation results, acquisitions were performed in two phantoms: a phantom constructed with the aim to include vials with different fat fractions (0.1, 0.2, 0.3, 0.4, 0.5) and a phantom composed of two regions, one of fat and one of gel solution (watery). All acquisitions were performed at Hospital da Luz, using Siemens AERA® 1.5 T MRI equipment, using a receiver head coil. The sequences used were predefined (cardiac sequences used by Siemens). The spatial variation of the ΔB0 field was also evaluated using a sequence already available in the equipment; in order to investigate its effect on the quantification of T1 with bSSFP.The simulations demonstrated the impact of fat partial volume and field heterogeneities on the estimated T1 value. Although the construction of a phantom composed of multiple vials with varying fat fractions proved too hard to provide reliable ground truth fat fraction values, the experiments were mostly consistent with the simulation study. The detected outliers could partly be related to errors in the experimental measurements of the fat fraction and field inhomogeneity. Future studies should investigate the impact of using a spoiled gradient echo readout instead of bSSFP and of applying signal models which include both the water and fat signal contributions.

Keywords: Cardiac Magnetic Resonance Imaging, MOLLI, Partial Volume Effect, Fat Fraction

1. Introduction

Cardiac magnetic resonance (CMR) has demonstrated its importance in the morphological and functional assessment of the heart, not only for the follow-up of pathologies, but also for the therapeutic decision. [1-2]

One of the emerging techniques in CMR is the mapping of the longitudinal relaxation time (T1) because it allows the characterization of myocardial tissue in a quantitative way, unlike other techniques such as delayed enhancement. Since the range of values for the T1 parameter in normal myocardium is known, variations of this parameter outside this range will indicate pathological changes. [3-5]

The most widely used technique in T1 parameter mapping is the modified Look-Locker Inversion recovery (MOLLI). [6] This allows overcoming limitations related to respiratory movement, through acquisition in a single apnea period, as well as the acquisition time, through the ability to obtain images with different inversion times (TI) after a single inversion pulse, called the Look-Locker method. [7] In MOLLI, a balanced steady-state free precession (bSSFP) reading is applied to maximize the signal-to-noise ratio (SNR) in a reduced image acquisition time, coinciding with the end of diastole to minimize cardiac motion artifacts. [6-8]

But this approach has been shown to be vulnerable to partial volume effects (PVE) that can arise due to fat infiltration. [9,10] In addition, the effect of fat on T1 estimates may differ in the presence of static B0 field heterogeneities (ΔB0). To improve the accuracy of the T1 estimates, this information can be measured separately and taken into account in its adjustment. [10,11]

The main objective of this project was to evaluate the impact of the presence of fat infiltration in the tissue on the quantification of myocardial T1. First, signal simulations of T1 inversion-recovery (IR) mapping sequences with bSSFP were performed, and the bias and accuracy of T1 estimates for different fat fractions and deviation from the nominal B0 field were evaluated. To validate the simulation results, phantom acquisitions were performed, including a multi-gradient echo sequence to measure ΔB0 and fat, in order to account for their effect on T1 quantification with bSSFP. An in-vivo test was also performed on one leg with the same purpose.

2. Background

2.1 Cardiac Magnetic Resonance

The application of MRI as a diagnostic method is due to the ability to assess and quantify different cardiac pathologies such as ischemia, cardiomyopathy and changes in ventricular function. This is a non-invasive method, increasingly applied in clinical practice due to its flexibility. [1,2] The main challenges in CMR are cardiac movement, blood flow, and respiratory movement. Artifacts may appear in images due to changes in signal strength or phase as a function of time. In the case of blood flow, depending on the applied pulse sequences, acquisition times and flow characteristics, different signals can be produced, as we are in the presence of a tissue that is not stationary.

When excitation occurs in the selected slice selection for imaging, signal acquisition may not be achieved because tissues are in motion. Artifacts arising due to cardiac movement are more effectively controlled by synchronizing the image acquisition with the patient's ECG so that all phase encodings are performed at exactly the same point in the cardiac cycle. For gating, a good quality ECG waveform is required for the MR system to detect the QRS complex and initiate acquisition – Figure 1.

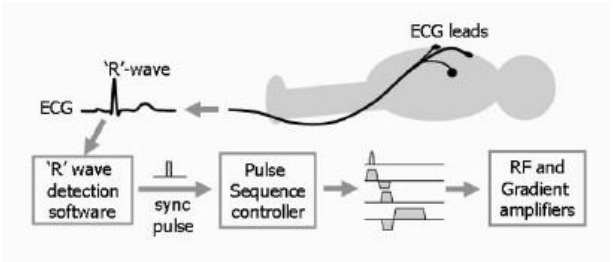

Figure 1 - ECG synchronization with image pulse sequence. Cardiac synchronization is achieved by obtaining the patient's ECG signal. A software algorithm is applied that detects the QRS complex and generates a synchronization pulse, which initiates the production of radio frequency and gradient pulse waves, which are amplified to drive the radio frequency transmitter and gradient coils. Adapted from [12]

2.1. T1 Mapping

T1 corresponds to the tissue's longitudinal relaxation time, which dictates the return of the longitudinal magnetization to its equilibrium value after the application of a radiofrequency (RF) pulse. For each tissue type, the values measured for the T1 relaxation time depend on the magnetic field strength (for healthy myocardium at 1.5 T, values between 900 and 1000 ms are common; for 3 T, they vary between 1000 and 1200 ms) , and any deviation from these intervals may indicate pathology. The T1 values that are measured can be influenced by a number of factors, such as age, heart rate, pathology, and the pulse sequences used.[13] The T1 mapping is based on the acquisition of several images with different T1 weights, being used to adjust the parameters that describe the signal evolution during the T1 relaxation process.[13,14] For the measurement of T1, the magnetization of The balance is inverted or suppressed, depending on the type of RF pulse applied, and the waiting time between the preparation pulse and acquisition of T1-weighted images is also variable.

The protocols currently applied are based on IR or saturation-recovery (SR). Images are acquired at different points on the recovery curve, and an independent pixel-by-pixel curve fit is performed to estimate a parametric map with T1 values at each spatial location. Images are usually acquired in the same phase of the cardiac cycle and in the same respiratory phase to eliminate movement and possible artifacts caused by it.

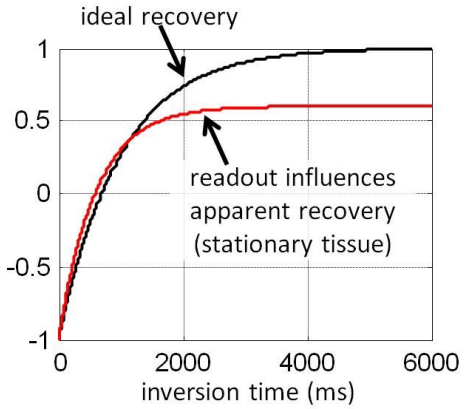

*Figure 2 - Apparent inversion recovery (T1 *) is influenced by the bSSFP reading. Effective inversion recovery is fitted using a 3-parameter model, and T1 is estimated using the Look-Locker correction. Adapted from [15]*

Currently, the most used technique in clinical practice for T1 mapping is MOLLI. [6] Through this technique, image data segments are acquired repeatedly after an inversion pulse, and several images are created along the recovery curve (Figure 2). The image acquisition is repeated after a period of the order of 5 * T1 in order to allow complete recovery of the longitudinal magnetization between Look-Locker cycles. One of the advantages of this technique is that it allows the acquisition of a large number of images for estimating T1 in a short time. However, without synchronization with cardiac movement, each image would correspond to a different phase of the cardiac cycle, so T1 mapping would not be possible. Furthermore, the RF pulses used to acquire the images themselves also affect the T1 recovery curve, so an apparent T1 (T1*) is actually measured (Figure 2). [15,16] With the application of this reading, an apparent recovery time denoted as T1* arises, which is less than the actual longitudinal recovery time, T1, which is the desired tissue parameter. As a result of the reading influence, the recovery inversion curve follows a 3-parameter exponential signal model:

$$S = A - Bexp\ (-\frac{t}{T1^*}) \qquad (1)$$

where A and B are parameters that relate to the equilibrium magnetization and the setup time, t represents the inversion time (time interval after setup), and T1 * is the apparent T1. [17,18] The 3-parameter model is fitted to measured values to estimate A, B and T1 * which can be used to obtain a rough estimate of T1 ≈ T1*× (B / A - 1). The derivation for the "Look-Locker" correction factor (B / A - 1) is based on a continuous reading through the Fast Low Angle SHot (FLASH) [19,20].

In this technique, single-shot images are obtained intermittently in diastole, introducing a three-cycle pause after image acquisition in the initial five heartbeats, in order to allow for magnetization recovery. The acquisition time can be further reduced using another technique: shortened modified Look-Locker (shMOLLI). The acquisition of shMOLLI is achieved using the 5(1)1(1)1 method (3 Look-Locker inversions over 9 heartbeats), in which, the last or the last two magnetization inversions may not be complete, depending on of T1. [21,22]

2.3 Partial Volume Effect

The longitudinal relaxation time constant (T1) of the myocardium varies according to the different stages of disease, due to the increase in the amount of water or other molecular changes. The detection of diseases at early stages by measuring T1 requires high reproducibility, which is limited by systematic errors. [23,24].

The partial volume effect occurs when the voxel in the myocardium also includes fat and/or blood. This effect may affect the estimation of the myocardial native T1 values when bSSFP sequences are used, since the fat and water signals may be in phase opposition; in this case the combined signal measured during magnetization recovery represents the difference rather than the sum of the two components. In the presence of this artifact, fat detection is restricted by the fraction of fat present in the voxel and by the size of the region that determines the contrast between fat and water. It is possible to estimate the fraction of water and fat through a gradient echo sequence with at least three echoes obtained so that water and fat are now perfectly in phase or in phase opposition (Dixon method), from which generates an image corresponding to the contribution of water and another of fat [25,26]. This technique allows the estimation of a positive contrast fat image that improves its detectability, but is limited by the SNR. Fat can also be identified on T1 maps, due to the low T1 fat, as long as the region has sufficient dimensions. When the fat fraction is reduced, it becomes difficult to interpret the estimated T1 of the voxels that contain water and fat combined. [27]

Typically, when using the MOLLI recovery sequence [6], a signal recovery model is used that assume the recovery of a single species, following a mono-exponential model. When this model is applied to a voxel that contains two components with different values of T1, an incorrect estimate of T1 is obtained because partial volume errors break the assumptions of current T1 mapping methods.

Voxels located at the tissue boundary between the myocardium and blood contains the partial volume of each of them and produces an estimated T1 that corresponds to an intermediate value between blood and myocardium in proportion to their quantity. However, when the voxels contain both fat and myocardium, the estimated T1 value may be higher than the T1 values of both fat and myocardium, which may cause an artifactual progression of T1. This phenomenon is related to the use of bSSFP readings, since in many of these protocols, the fat and water components are in phase opposition.

3. Materials and Methods

3.1. Simulations

In the MATLAB® software, signal simulations of the IR T1 mapping sequences were performed with bSSFP and the accuracy of the T1 estimates was compared for different fat fractions. The simulations were carried out to investigate the behavior of these sequences (accuracy and precision of estimated T1) in different contexts, having been familiarized with the developed code, which allowed the realization of several adjustments and corrections, in order to be fully adjusted to specific needs of the study

The values of T1 were obtained by making a curve fit given by the equation S=A-Bexp (-t/T1*).

The adjustment of the model for estimating T1 was performed using the lsqcurvefit function with the trust-region-reflective algorithm, with a residue stop criterion less than 1e-6 or maximum 100 iterations, having as initial parameters A=1, B=2 , T1 =1000 ms.

Bloch equation simulations of the MOLLI sequence were performed with typical parameters: repetition time of 2.65 ms (TR), initial inversion time of 110 ms (TI), T1 of 1000 ms, T2 of 45 ms, SNR of 40 and 35º flip angle. In these simulations the tested fat fraction (FF) values were 0:0.01:1.

A sampling scheme of 5(3)3 was chosen, with RR of 1000 ms (60 bpm). The simulations were performed with a static B0 field ranging between – 377 and 377 Hz (-1/TR, 1/TR) and FF between 0 and 1.

3.2. Experimental Validation

3.2.1 Construction of the Phantoms

The realization of the phantom comprised two stages: the production of a bottom zone, corresponding to water, and the production of different fat fractions (0.1, 0.2, 0.3, 0.4, 0.5). For the bottom zone, was added to 500 ml of pre-warmed water, 50 grams of agar-agar. After placing on a magnetic stirrer with analogue heating, the mixture was subjected to heating so as to boil for about 30 minutes. The preparation was then deposited in an appropriate container for acquisition in the MR equipment. The entire mixture was carefully shaken so that it became homogeneous. After about 60 minutes of rest at room temperature, the phantom was placed in the refrigerator until it was semi-solid (about 3 hours).

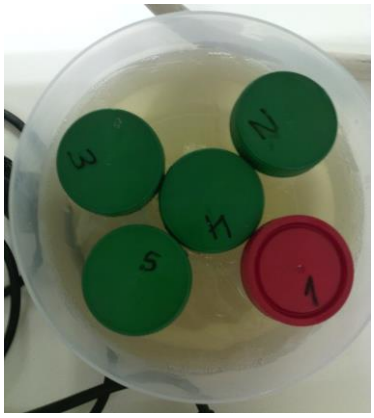

Figure 3 - Phantom with different fat fractions (FF). Each vial corresponds to the following fractions 0.1, 0.2, 0.3, 0.4, 0.5.

Later, another phantom of water and fat was created, composed of two regions: one containing water and agar-agar, doped with other substances in order to present relaxation times closer to the myocardial tissue, and the other just fat (Figure 4). This phantom comprised 175 ml of water and the following reagents: Gel: 2% w/v agar-agar, ionic equilibrium: 43 mm NaCl, T1 contrast: nickel (II) hexahydrate. The use of this phantom allows the generation of an interface region with partial volume, through the selection of an angled slice when acquiring MR images.

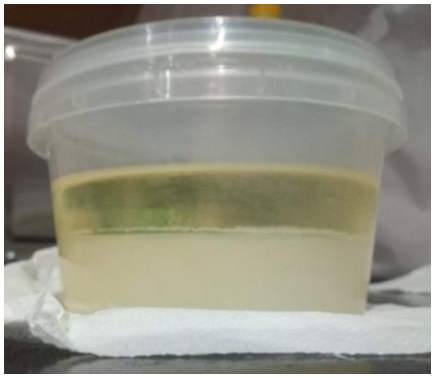

Figure 4 - Phantom Interface, composed of two regions: fat and a gel solution (agarosa)

3.2.2 Acquisitions and MRI and image analysis

To validate the simulation results, phantom acquisitions were performed, including a gradient echo sequence with multiple echoes to measure T2* and fat. The spatial variation of the ΔB0 field was evaluated using a sequence already available in the equipment in order to explain their effect on the quantification of T1 with bSSFP.

In the present study, all acquisitions were carried out at Hospital da Luz.

The images were acquired between September 2020 and February 2021, using Siemens AERA® 1.5 T RM equipment, using a skull coil. The sequences used were predefined (cardiac sequences used by Siemens), only with the alteration of some protocols and some acquisition parameters.

The acquisitions were made using the two phantoms.

All images were exported from the acquisition equipment in DICOM format.

The Image Processing was carried out through a DICOM image visualization application, the RadiAnt DICOM Viewer. To perform the segmentation, a standard size for the ROI was defined, which was unchanged throughout the study (ellipse ROI with an area of 0.9012cm2). An ROI was placed in different portions of each vial, without covering the boundary region of the same (Figure 5). These markings were performed on all five flasks on T1-weighted images, GRE sequence, T1 Mapping and Dixon (fat-only and water-only).

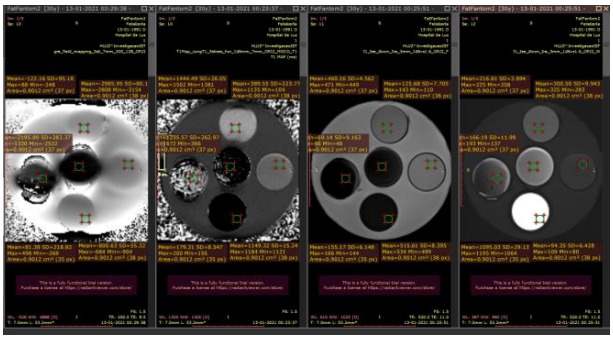

Figure 5 - Representation of the location of the ROIs of 0.9012 cm^2 in a central section of the phantom of the 5 vials (vial 1 corresponds to the lowest ROI, vial 2 corresponds to the leftmost ROI, vial 3 corresponds to the highest ROI, vial 4 corresponds to the ROI located in the center, vial 5 to the rightmost ROI)

In the Interface phantom, vertical and horizontal ROIs were marked, as shown in Figure 6. To mark these ROIs, regions where there was variation in the fat fraction, regions that only contained water and regions that only contained fat were covered.

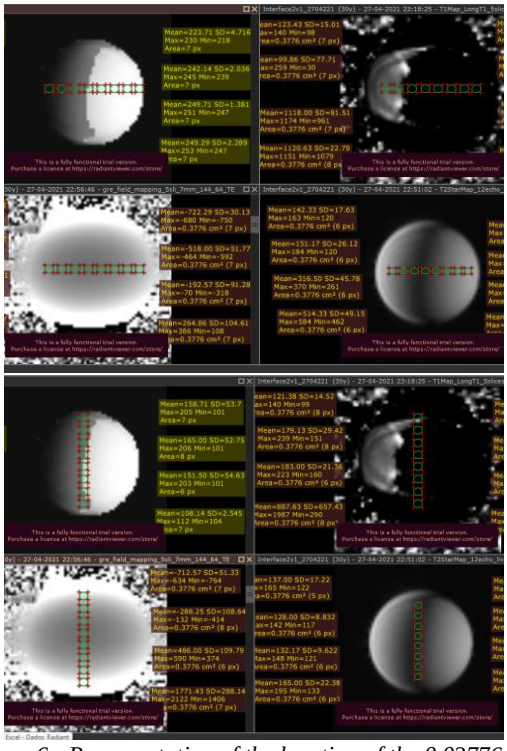

Figure 6 - Representation of the location of the 0.03776 cm^2 ROIs in a central section of the Horizontal and Verticals Interface

Additionally, an in vivo acquisition was performed on a leg (Figure 7), in order to evaluate the observations made in the simulations and in the phantoms, instead of being performed on the heart, to avoid the added difficulty of dealing with the movements associated with the cardiac cycles and breathing.

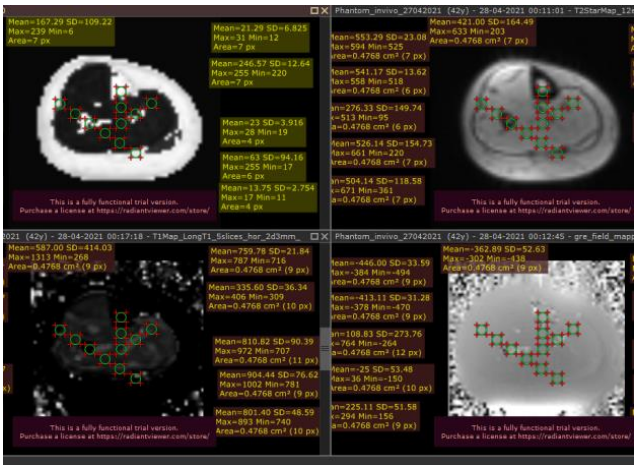

Figure 7 - Representation of the location of ROIs of 0.4768 cm^2 in a central cut of the Invivo acquisition of the leg, covering regions where there was variation in the fat fraction

In the case of the interface phantom and in vivo acquired images, the fat fraction was estimated not from Dixon images, but using a multi-echo GRE sequence similar to that proposed by O'Regan et al [32]. The echo times used for the image sequence were chosen so that the water and grease signals were approximately in-phase and in opposition to phase, so that an oscillation pattern in the signal was visible. To estimate the FF fat fraction, the two contributions (water and fat) were considered taking into account their difference in the resonant frequency ($\Delta\omega$=210Hz at 1.5T), and fixing the corresponding T2* values after their estimation using a model with a single signal component in sections containing only water or fat (T2*F=15ms and T2*W=60ms) - Figure 8:

$$|S(t)|/\max|S(t)| = \left|(1-\mathrm{FF})e^{-t/T2^*_W} + FFe^{-t/T2^*_F + i\Delta\omega t}\right| \quad (2)$$

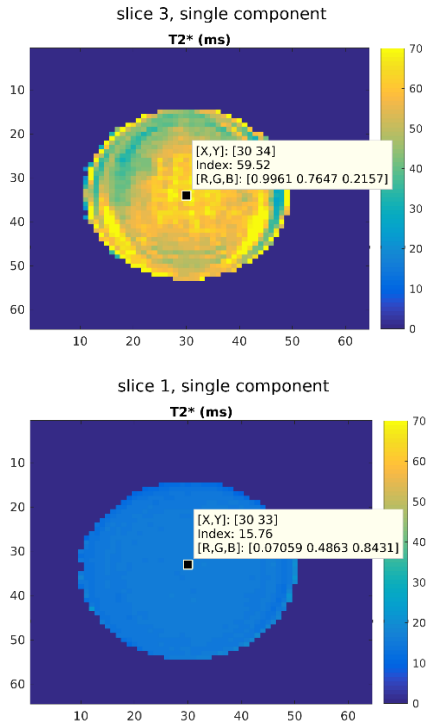

Figure 8 - Estimated T2 values for the agar-agar (on top) and fat (below) component measured in sections where there was only one component.*

The adjustment of this model was made with the lsqcurvefit function of Matlab, using the trust-region-reflective algorithm, with a residue stop criterion less than 1e-6 or maximum 100 iterations, having as an initial parameter FF=0.9 and keeping the too fixed.

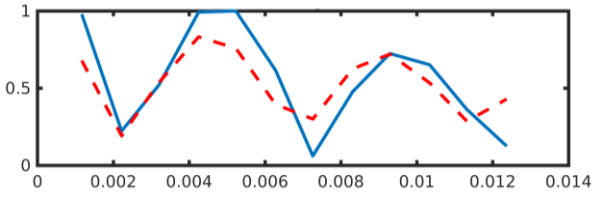

Figure 9 - Example of adjustment to determine the FF fat fraction: in blue an experimental curve is shown for a pixel containing water and fat and in red the theoretical curve obtained after the adjustment.

The ROIS mean and standard deviation values were taken directly from the RadiAnt DICOM Viewer program. To calculate the fat fraction from the images of water and fat obtained through the Dixon acquisition, the expression FF = SF/(SW+SF) was applied.

The error estimation for FF was calculated using the equation, where w corresponds to SW and f to SF:

$$\delta_{FF}^2 \approx \left(\frac{\partial FF}{\partial w}\right)^2 \delta_w^2 + \left(\frac{\partial FF}{\partial f}\right)^2 \delta_f^2$$

$$= \left(-\frac{f}{(f+w)^2}\right)^2 \delta_w^2 + \left(\frac{w}{(f+w)^2}\right)^2 \delta_f^2 \qquad (3)$$

$$\delta_{FF}^2 \approx \left(-\frac{SF}{(SF+SW)^2}\right)^2 \delta_w^2 + \left(\frac{SW}{(SF+SW)^2}\right)^2 \delta_F^2$$

4. Results and Discussion

4.1. Simulations

With the variation of B0, the T1 values remain constant (between 200 and 1000 ms) depending on the FF fat fraction, with only a few regions where these T1 values double – Figure 10.

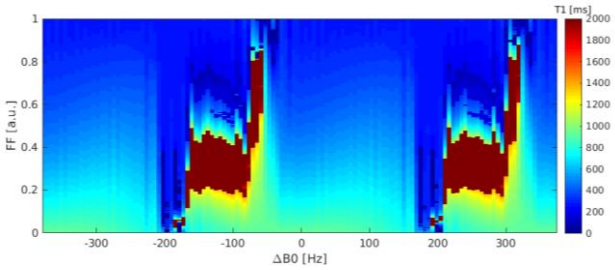

Figure 10 - Effect of T1 on the value of B0 in the presence of fa

As can be seen in Figure 10, for a ΔB0 that comprises values between -200 and 50 Hz and for a FF between 0.1 and 0.8, the highest values of T1 are reached (>1800ms). The same is true for a ΔB0 which comprises values between 200 and 340 Hz.

4.2. Experimental Validation

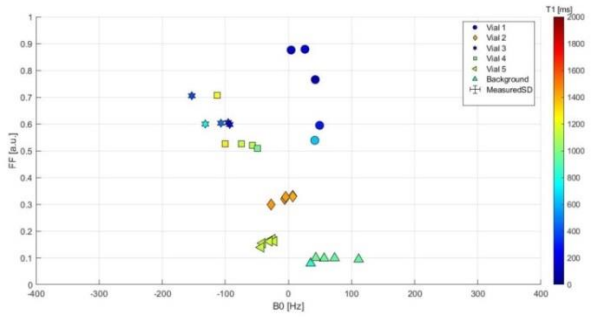

Figure 11 - Results obtained for the values of B0 and FF with the variation of T1, in the acquisition of the Phantom for the respectives vials and background

With regard to vial 1, it was possible to identify that there was a greater difference in values in terms of FF than in relation to B0, that is, while the FF values varied between roughly 0.5 and 0.9., the B0 values registered if between 0 and approximately 50 Hz. Such discrepancy may have been caused by errors that occurred during the construction of the phantom and the manipulation of the reagents in its constitution. It should also be noted that in terms of T1, the values remained relatively constant, having been 200 ms and in only one of the cases it recorded 600 ms.

With regard to vial 2, it is possible to see that in the 5 times tested, the values obtained remained fairly constant. With regard to FF, they only ranged between 0.3 and 0.35., and in terms of B0 they ranged between -50 and 25 Hz, appreciably. In terms of T1, they always recorded constant

values of approximately 1500 ms.

In relation to vial 3, it is possible to notice that there was little variation in values. With respect to FF, these ranged between 0.6 and 0.7., and in relation to B0, they ranged between -250 and -85 Hz, appreciably. T1 for its part three times maintained constant values of 200 ms, and twice values of 600 ms, approximately.

In vial 4, a situation identical to vial 3 occurred, recording identical results 4 times and only one of them taking different values from the others. Regarding the FF values, they ranged between 0.5 and 0.7., while those of B0 ranged between -125 and -40 Hz, approximately. Regarding T1, there were also discrepancies in values ranging between 600 and 1200 ms.

Vial 5 values were the ones that assumed the most identical results. In terms of FF, they only varied between 0.125 and 0.195, approximately, and in relation to B0 they oscillated between -25 and -50 Hz, appreciably. The t1 for all cases in vial 5 assumed values of 1000 ms.

In relation to the Fund, these assumed quite identical values in terms of FF, approximately 0.1, and in terms of B0 they varied between 30 and 120 Hz. As regards T1, they assumed values of 800 ms.

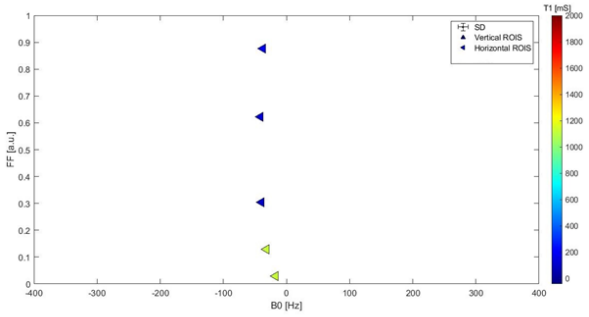

Figure 12 - Results obtained for the values of B0 and FF with the variation of T1, in the Phantom Interface (vertical and horizontal ROIS)

Regarding the acquisition of the interface phantom, it is possible to see that only five of the eight horizontal ROIs are present in this graphical representation. Since the values of T1, present a greater variation for values below and above the FF 0.2, values of 1100 ms and 200 ms, respectively. For all points there was no significant variation of B0, considering that the values were relatively low, between -50 and 0 Hz.

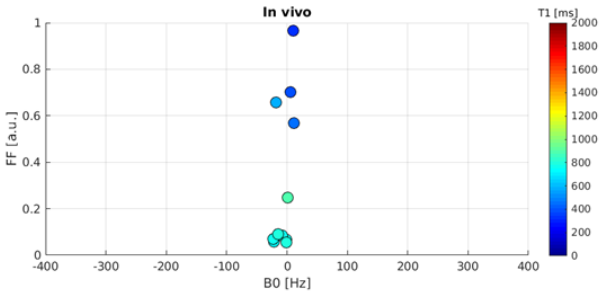

Figure 13 - Results obtained for the values of B0 and FF with the variation of T1, in the Invivo acquisition

In reality concerning the Invivo acquisition, it is possible to identify two distinct regions with importance forming clusters. Despite having used a reduced spatial resolution to try to force the occurrence of PVE, the low variation of the B0 value allowed to avoid the destructive interference of water and fat contributions.

In relation to the possible groups to be identified, one of them registered relatively lower B0 values, namely between -30 and 0 Hz. This same group obtained FF values between 0.05 and 0.1 and 800 ms in terms of T1. approximately corresponding to muscle.

In the second grouping, it was possible to distinguish that the B0 values varied between -30 and 20 Hz significantly, and in terms of FF they ranged between 0.55 and 0.75 approximately, more consistent with adipose tissue. In terms of T1 they got 400 ms.

Taking into account all the results obtained, it was possible to verify that for the simulations and acquisitions there are significant differences in the same vials, which should have similar FF. However, as described in the same subchapter, Outliers were detected. These were probably due to errors in the construction of the phantom, in the measurements of its reagents during its construction, in the constitution of the different fat fractions and in the solidification of the agar, which may be behind some heterogeneities in the FF value observed in some of the vials. In particular, the solidification of the agar was in most cases not fast enough to avoid the separation of the two phases, water and fat, constituents of each vial.

Another limitation is that images of the heart were not acquired. The difficulty would be to obtain the measurement of fat in the same cardiac cycle and with the sequences we had, the only way to do it would be separately, being difficult to guarantee that it would correspond to the same anatomical region. Patient-related factors such as heart rate and respiratory movement can affect the measurement, loss of spatial resolution due to movement, increasing the occurrence of partial volume effect.

On the other hand, it would be important to implement the use of models in which FF is distinguished, namely explicitly considering its contribution to the signal measured with the MOLLI sequence for mapping the constant T1.

5. Conclusions

The measurement of myocardial T1 using current T1 mapping methods using b-SSFP protocols is subject to bias when a mixture of myocardial tissue and fat occurs. The partial volume effect in the heart occurs at the tissue boundaries and in cases where there is intramyocardial fat. It is important to understand this mechanism as it can lead to misinterpretations.

This work focused on evaluating the impact of the presence of fat infiltration in the tissue on the quantification of myocardial T1. Through the simulations and their comparison with the acquisitions in phantoms and invivo, it was possible to verify the influence that the different fat fractions and B0 variations have on the T1 values.

For future work, an attempt should be made to include FLASH simulations and acquisitions, since this sequence is known to be more robust to B0 variations and to attenuate artifacts originating from out-of-resonance signal, compared to bSSFP, and it would be interesting to compare them. It would also be relevant to test the application of models that allow considering simultaneously the contribution of water and fat in the measured signal and, consequently, in the estimated T1 value.

Finally, it would also be interesting to perform acquisitions in MRI equipment with a magnetic field strength greater than 1.5 T. By doubling the magnetic field strength from 1.5 T to 3 T, we doubled the frequency variations within and around the heart that occur due to differences in susceptibility and, consequently, we increase the possibility that some regions of the image have a frequency out of band of the SSFP. The T1 relaxation time depends on the field strength with a significant increase in T1 from 1.5 T to 3 T. Higher field strength has some advantages and disadvantages in quantifying myocardial T1. A disadvantage is a greater inhomogeneity of the B0 field, which induces variations in the apparent T1. However, a higher field strength provides a higher SNR, which can be exchanged by decreasing the errors associated with the B0 variation, by decreasing the repetition time (TR).

Acknowledgments

This document was written and made publically available as an institutional requirement and as part of the evaluation of the MSc thesis in Bioengineering and Nanosystems of the author at Instituto Superior Técnico. The work described herein was developed at Evolutionary Systems and Biomedical Engineering Lab of Instituto Superior Técnico (Lisbon, Portugal) in collaboration with Hospital da Luz during the period September 2020 - May 2021, under the supervision of Prof. Dr. Rita Nunes and Eng. Andreia Gaspar.

References.

1. Peterzan MA. Rider OJ. Anderson LJ. “The Role of Cardiovascular Magnetic Resonance Imaging in Heart Failure”. *Card Fail Rev*. 2016; 2(2):115– 122.
2. Doesch, C., Papavassiliu, T. Diagnosis and management of ischemic cardiomyopathy: Role of cardiovascular magnetic resonance imaging. World journal of cardiology. 2014; 6(11): 1166–74
3. Ferreira VM. Piechnik SK. Dall’Armellina E et al. “Native T1-mapping detects the location, extent and patterns of acute myocarditis without the need for gadolinium contrast agents”. *J Cardiovasc Magn Reson*. 2014; 16(36).
4. Mewton N. Liu C.Y. Croisille P. Bluemke D. Lima J.A. “Assessment of myocardial fibrosis with cardiovascular magnetic resonance”. *JACC*. 2011; 57: 891-903
5. Puntmann V.O. Nagel E. “T1 and T2 mapping in nonischemic cardiomyopathies and agreement with endomyocardial biopsy”. *JACC*. 2016; 68: 1923-1924
6. Messroghli DR, Radjenovic A, Kozerke S, et al. “Modified Look-Locker inversion recovery (MOLLI) for high-resolution T1 mapping of the heart”. *Magn Reson Med* 2004; 52:141-6
7. Nacif Nacif MS, Turkbey EB, Gai N, et al. “Myocardial T1 mapping with MRI: Comparison of look-locker and MOLLI sequences”. *J Magn Reson Imaging*. 2011; 34:1367–1373
8. Messroghli DR, Plein S, Higgins DM, et al. “Human myocardium: single-breath-hold MR T1 mapping with high spatial resolution--reproducibility study”. *Radiology* 2006; 238:1004-12
9. Mozes FE, Tunnicliffe EM, Moolla A, Marjot T, Levick CK, Pavlides M, et al. “Mapping tissue water T1 in the liver using the MOLLI T1 method in the presence of fat, iron and B0 inhomogeneity”. *NMR Biomed*. 0(0):e4030.
10. Marty B, Carlier PG. “Physiological and pathological skeletal muscle T1 changes quantified using a fast inversion-recovery radial NMR imaging sequence”. *Sci Rep*. 2019 May;9(1):6852.
11. Liu D, Steingoetter A, Parker HL, Curcic J, Kozerke S. “Accelerating MRI fat quantification using a signal model-based dictionary to assess gastric fat volume and distribution of fat fraction”. *Magn Reson Imaging*. 2017;37:81–9.
12. Ridgway JP. “Cardiovascular magnetic resonance physics for clinicians: part I.” *J Cardiovasc Magn Reson*. 2010;12(1):71.
13. H Messroghli DR, Greiser A, Frohlich M, et al. “Optimization and validation of a fully-integrated pulse sequence for modified look-locker inversion-recovery (molli) T1 mapping of the heart”. *J Magn Reson Imaging* 2007; 26:1081-6.
14. Moon JC, Messroghli DR, Kellman P, et al. “Myocardial T1 mapping and extracellular volume quantification: a Society for Cardiovascular Magnetic Resonance (SRMC) and RMC Working Group of the European Society of Cardiology consensos statement”. *J Cardiovasc Magn Reson* 2013; 15:92.
15. Kellman, P., Hansen, M.S. T1-mapping in the heart: accuracy and precision. *J Cardiovasc Magn Reson. 2016;* 16(2)

16. Iles L, Pfluger H, Phrommintikul A, Cherayath J, Aksit P, Gupta SN, Kaye DM, Taylor AJ: "Evaluation of diffuse myocardial fibrosis in heart failure with cardiac magnetic resonance contrast-enhanced T1 mapping". *J Am Coll Cardiol*. 2008, 52: 1574-80
17. Chow K, Flewitt JA, Green JD, Pagano JJ, Friedrich MG, Thompson RB. "Saturation recovery single-shot acquisition (SASHA) for myocardial T1 mapping". *Magn Reson Med*. 2014; 71:2082–2095.
18. Kim, Pan & Hong, Yoo & Im, Dong & Suh, Young Joo & Park, Changhun & Kim, Jin & Chang, Suyon & Lee, Hye-Jeong & Hur, Jin & Kim, Young & Choi, Byoung Wook. "Myocardial T1 and T2 Mapping: Techniques and Clinical Applications*". Korean Journal of Radiology*.2017; 18(1): 113–131
19. Nekolla S, Gneiting T, Syha J, Deichmann R, Haase A. "T1 maps by k-space reduced snapshot-FLASH MRI". *J Comput Assist Tomogr* 1992; 16:327–332.
20. Deichmann R, Haase A: "Quantification of Tl Values by SNAPSHOT-FLASH NMR Imaging". *J Magn Reson.* 1992, 612: 608-12.
21. Robson MD, Piechnik SK, Tunnicliffe EM, Neubauer S. "T1 measurements in the human myocardium: The effects of magnetization transfer on the SASHA and MOLLI sequences*". Magn Reson Med* 2013; 670:664–670.
22. Kellman P, Herzka DA, Arai AE, Hansen MS." Influence of off resonance in myocardial T1-mapping using SSFP based MOLLI method". *J Cardiovasc Magn Reson* 2013; 15:63
23. Tran-Gia J, Wech T, Hahn D, Bley TA, Köstler H. "Consideration of corte profiles in inversion recovery Look-Locker relaxation parameter mapping". *Magn Reson Imaging*. 2014; 32:1021–30
24. Rodgers CT, Piechnik SK, DelaBarre LJ, et al. "Inversion recovery at 7 T in the human myocardium: measurement of T1, inversion efficiency and B11". *Magn Reson Med* 2013; 70:1038–1046.
25. Moon JC, Messroghli DR, Kellman P, Piechnik SK, Robson MD, Ugander M, et al. "Myocardial T1 mapping and extracellular volume quantification: a Society for Cardiovascular Magnetic Resonance (SRMC) and RMC Working Group of the European Society of Cardiology consensus statement". *J Cardiovasc Magn Reson*. 2013;15:92.
26. Higgins DM, Moon JC. "Review of T1 Mapping Methods: Comparative Effectiveness Including Reproducibility Issues". *Curr Cardiovasc Imaging Rep*. 2014;7:9252.
27. Kellman P, Hernando D, Arai AE. Myocardial Fat Imaging. Curr Cardiovasc Imaging Rep. 2010;3:83–91
28. Reeder SB, Markl M, Yu H, Hellinger JC, Herfkens RJ, Pelc NJ. "Cardiac CINE imaging with IDEAL water-fat separation and steady-state free precession". *J Magn Reson Imaging*. 2005;22:44–52.
29. Ferreira VM, Holloway CJ, Piechnik SK, Karamitsos TD, Neubauer S. "Is it really fat? Ask a T1-map*". Eur Heart J Cardiovasc Imaging*. 2013;14(11):1060
30. Bull S, White SK, Piechnik SK, Flett AS, Ferreira VM, Loudon M, et al. "Human non-contrast T1 values and correlation with histology in diffuse fibrosis". *Heart.* 2013;99:932–7.
31. Ugander M, Bagi PS, Oki AJ, Chen B, Hsu L-Y, Aletras AH, et al. "Myocardial edema as detected by pre-contrast T1 and T2 RMC delineates area at risk associated with acute myocardial infarction". *JACC Cardiovasc Imaging*. 2012;5:596–603
32. O'Regan DP, Callaghan MF, Fitzpatrick J, Naoumova RP, Hajnal JV, Schmitz SA. "Cardiac T2* and lipid measurement at 3.0 T-initial experience". *Eur Radiol*. 2008 Apr;18(4):800-5.